

---

# MicroRNA-130a can inhibit hepatitis B virus replication via targeting PGC1 $\alpha$ and PPAR $\gamma$

---

JYUN-YUAN HUANG,<sup>1,2</sup> SHU-FAN CHOU,<sup>2,3</sup> JUN-WEI LEE,<sup>2</sup> HUNG-LIN CHEN,<sup>2</sup> CHUN-MING CHEN,<sup>2</sup> MI-HUA TAO,<sup>2</sup> and CHIAHO SHIH<sup>1,2</sup>

<sup>1</sup>Graduate Institute of Life Sciences, National Defense Medical Center, Taipei, 114 Taiwan

<sup>2</sup>Institute of Biomedical Sciences, Academia Sinica, Taipei, 115 Taiwan

<sup>3</sup>Graduate Institute of Microbiology, College of Medicine, National Taiwan University, Taipei, 110 Taiwan

## ABSTRACT

In hepatitis B virus (HBV)-replicating hepatocytes, miR-130a expression was significantly reduced. In a reciprocal manner, miR-130a reduced HBV replication by targeting at two major metabolic regulators PGC1 $\alpha$  and PPAR $\gamma$ , both of which can potently stimulate HBV replication. We proposed a positive feed-forward loop between HBV, miR-130a, PPAR $\gamma$ , and PGC1 $\alpha$ . Accordingly, HBV can significantly enhance viral replication by reducing miR-130a and increasing PGC1 $\alpha$  and PPAR $\gamma$ . NF- $\kappa$ B/p65 can strongly stimulate miR-130a promoter, while miR-130a can promote NF- $\kappa$ B/p65 protein level by reducing PPAR $\gamma$  and thus NF- $\kappa$ B/p65 protein degradation. We postulated another positive feed-forward loop between miR-130a and NF- $\kappa$ B/p65 via PPAR $\gamma$ . During liver inflammation, NF- $\kappa$ B signaling could contribute to viral clearance via its positive effect on miR-130a transcription. Conversely, in asymptomatic HBV carriers, persistent viral infection could reduce miR-130a and NF- $\kappa$ B expression, leading to dampened inflammation and immune tolerance. Finally, miR-130a could contribute to metabolic homeostasis by dual targeting PGC1 $\alpha$  and PPAR $\gamma$  simultaneously.

**Keywords:** hepatitis B virus; microRNA; PGC1 $\alpha$ ; PPAR $\gamma$ ; inflammation

## INTRODUCTION

Human hepatitis B virus (HBV) is a very common human pathogen. To date, it remains a challenge to completely eradicate HBV in chronic hepatitis B patients. Chronic infection with HBV leads to the development of hepatocellular carcinoma (HCC). MicroRNA (miRNA) is known to play an important regulatory role in differentiation, development, and infectious diseases (Ambros 2011). Many HCC-related microRNAs have been reported (Liu et al. 2011; Szabo and Bala 2013); however, the roles of microRNAs in liver physiology and pathology have remained to be explored.

Liver enriched transcription factors and coactivators have been studied for their effect on HBV enhancer/promoter, including HNF1, HNF4 $\alpha$ , C/EBP $\alpha$ , PPAR $\alpha$ , and PGC1 $\alpha$  (Quasdorff and Protzer 2010; Bar-Yishay et al. 2011). In the case of PGC1 $\alpha$  coactivator, it can stimulate many transcription factor partners (Finck and Kelly 2006). In addition to promoting hepatic gluconeogenesis (Yoon et al. 2001), PGC1 $\alpha$  is known to be involved in adaptive thermogenesis in brown adipose tissue (Puigserver et al. 1998), mitochondria biogenesis, and respiration (Houten and Auwerx 2004), as well as neurodegenerative diseases (St-Pierre et al.

2006). Furthermore, PGC1 $\alpha$  can activate HBV transcription and replication in hepatocytes (Shlomai et al. 2006; Ondracek et al. 2009; Ondracek and McLachlan 2011). Recently, microRNAs have emerged as an important posttranscriptional regulator of metabolism (Dumortier et al. 2013). It remains to be investigated whether HBV could have an effect on liver metabolism via microRNAs, and conversely, whether metabolism-related microRNAs could have an effect on HBV replication.

We report here that miR-130a can reduce HBV RNA transcription and DNA replication by targeting at the 3' UTRs of both PGC1 $\alpha$  and PPAR $\gamma$ , respectively. Cotransfection with the combination of PGC1 $\alpha$  and PPAR $\gamma$  expression vectors had a striking stimulatory effect on HBV replication. Furthermore, HBV replication can increase the levels of PGC1 $\alpha$  and PPAR $\gamma$  by reducing the endogenous level of miR-130a. Finally, we identified NF- $\kappa$ B/p65 as a positive transcription factor for miR-130a promoter. NF- $\kappa$ B is known to be involved in multiple biological functions, including inflammation, immune response, apoptosis, cell proliferation, and

© 2015 Huang et al. This article is distributed exclusively by the RNA Society for the first 12 months after the full-issue publication date (see <http://rnajournal.cshlp.org/site/misc/terms.xhtml>). After 12 months, it is available under a Creative Commons License (Attribution-NonCommercial 4.0 International), as described at <http://creativecommons.org/licenses/by-nc/4.0/>.

---

Corresponding author: [cshih@ibms.sinica.edu.tw](mailto:cshih@ibms.sinica.edu.tw)

Article published online ahead of print. Article and publication date are at <http://www.rnajournal.org/cgi/doi/10.1261/rna.048744.114>.

cancer development (Hayden and Ghosh 2004; Karin 2006). Taken together, we established two positive feed-forward loops here. The first positive loop is between HBV and PGC1 $\alpha$  and PPAR $\gamma$  via miR-130a. The second positive loop is between NF- $\kappa$ B/p65 and PPAR $\gamma$  via miR-130a. Since miR-130a is strategically positioned at the intersection of these two loops, it is very likely that miR-130a plays an important role in the communication between the first loop of liver metabolism and the second loop of liver inflammation. In HBV infected hepatocytes in chronic hepatitis B carriers, miR-130a is involved in a signaling circuitry which could mediate hepatic homeostasis. We discussed here the potential clinical significance of our studies.

## RESULTS

### Identification of anti-HBV cellular microRNAs

To look for potential changes in the expression of cellular miRNAs in HBV infected hepatocytes, we used the approach by microRNA microarray (Table 1). Previously, we established HBV-producing hepatoma cell lines which can produce virions infectious in chimpanzees (Shih et al. 1989, 1990). We compared microRNA expression profiles between stable HBV-producing and control cell lines by qPCR microarray (Materials and Methods), and observed significant reduction of at least a dozen miRNAs in HBV-producing rat hepatoma cells from a sub-library containing a total of 381 rat specific microRNAs (Table 1; Materials and Methods). The reduction of these miRNAs from this microarray study was validated by the stem-loop qPCR analysis (Fig. 1A). We noted that some of these reduced miRNAs were found in common in several independently established rat (Table 1) and human HBV-producing cell lines (data not shown). We speculated the possibility that at least some (not all) of these reduced microRNAs, may have a direct or indirect negative effect on HBV replication in hepatocytes. Using cotransfection and viral replication assays, we identified miR-130a and another microRNA (data not shown), which behaved antagonistic to HBV, from among a total of 12 microRNAs identified by the microarray analysis (Table 1). Therefore, >15% (2/12) of these microRNAs with reduced expression were found to inhibit HBV replication, when these HBV-inhibitory microRNAs were over-expressed. It remains to be further investigated whether such a microarray approach can be used as a general method to provide a short list of candidate miRNAs (12 out of 381) with an anti-vi-

ral potential. Here, we focused our studies only on miR-130a in this paper. The rest of the miRNAs in Table 1, including miR-31, had no significant effect on HBV replication (data not shown). By next-generation sequencing technique, we estimated that miR-130a alone exists at ~0.033% of the total microRNA population in a rat hepatoma cell line Q7-Neo (data not shown). Because miR-130a and miR-130b share the same seed sequences, we estimated that the abundance of miR-130a and miR-130b should be ~0.13% of the total microRNA population in Q7-Neo.

### Viral replication and gene expression attenuated by miR-130a

As shown in Figure 1B, a plasmid expressing miR-130a inhibited HBV DNA replication in human hepatoblastoma HepG2 cells. Furthermore, Northern blot analysis of total cytoplasmic RNA from the cotransfected culture revealed that miR-130a reduced the level of 3.5 kb HBV pregenomic RNA (pgRNA) and 2.4/2.1 kb subgenomic RNAs (Fig. 1C). The reduction of HBV DNA and RNA syntheses by miR-130a was confirmed by the reduction of HBV protein expression by Western blot analysis of intracellular HBV core protein (HBc) (Fig. 1D), and by ELISA of HBV surface antigen (HBsAg) and e antigen in the medium (HBeAg) (Supplemental Fig. S1).

Bioinformatic analysis predicted potential target sites of miR-130a clustering between nucleotide 1521 and nucleotide 2122 of HBV *ayw* genome (Fig. 1E, upper panel; Galibert et al. 1979). This region coincides with the 3' UTR of HBsAg, HBeAg, and HBc-specific RNAs (Tiollais et al. 1985; Yang et al. 2014). We performed the 3'-UTR luciferase reporter

**TABLE 1.** Q-PCR microarray of cellular microRNAs in HBV-producing and control hepatoma cell lines

miRNA	Fold change <sup>a</sup>				Average
	Qs2 <sup>c</sup>	Qs4 <sup>c</sup>	Qs5 <sup>c</sup>	Qs21 <sup>c</sup>	
rno-miR-222	-34,267	-32,467	-16,233	-32,467	-25,974
rno-miR-10a	-645.16	-465.12	-141.44	-518.13	-314.96
rno-miR-204	-383.14	-281.69	-301.2	-324.68	-310.47
rno-miR-187	-167.22	-119.33	-125.31	-139.28	-135.50
rno-miR-342	-110.90	-86.96	-88.50	-97.09	-96.53
rno-miR-31	-78.74	-37.31	-25.13	-121.36	-45.69
rno-miR-181a	-34.13	-25.64	-25.64	-29.33	-28.29
rno-miR-196c	-10.38	-13.09	-12.03	-11.57	-11.69
rno-miR-9	-15.92	-12.70	-13.73	1.69	-10.15
rno-miR-202-3p	-9.91	1.89	-9.99	-7.83	-7.40
rno-miR-195	-8.62	1.44	-9.13	-8.74	-6.26
rno-miR-130a <sup>b</sup>	-4.67	-3.86	-8.33	-7.63	-5.52

<sup>a</sup>The fold changes of the expression of miRNA in Qs2, Qs4, Qs5, Qs21 were normalized to the control cell lines Q7 neo.

<sup>b</sup>The results of miR-130a were confirmed by stem-loop real-time PCR analysis using HBV-producing human hepatoma cell lines UP7-4 and UP7-7 (Fig. 1A; Chen et al. 2012).

<sup>c</sup>Qs2, Qs4, Qs5, and Qs21 are infectious HBV-producing rat hepatoma cell lines (Shih et al. 1989, 1990).

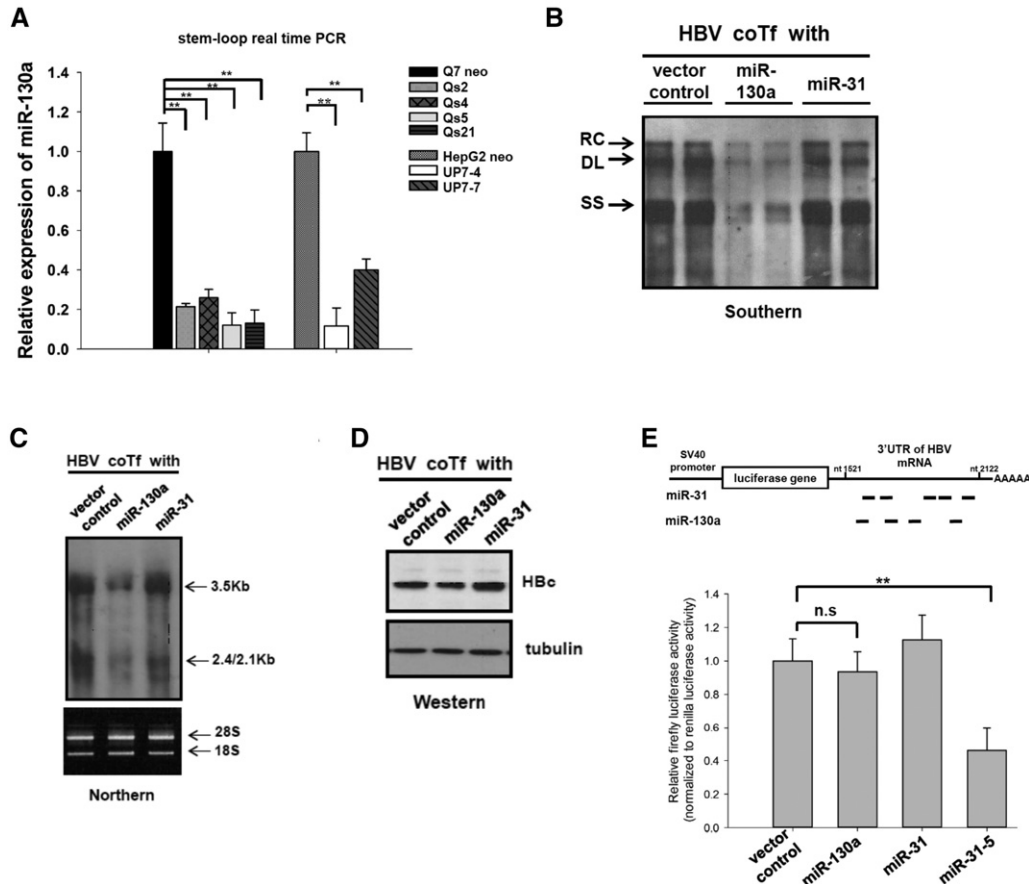


**FIGURE 1.** Human miR-130a can attenuate HBV replication and gene expression. (A) The expression level of miR-130a was always significantly reduced in stable HBV-producing cell lines. (B) Intracellular HBV replication using Southern blot assay in HepG2 cells were significantly reduced by cotransfection (coTf) of an HBV *ayw* genomic dimer plasmid and various miRNA expression vectors. The result here is representative of at least three independent experiments. The probe used here is a 2.8-kb HBV-specific DNA fragment containing HBV core gene. Empty vector control and miR-31 were included as negative controls. HBV replicative intermediates: (RC) relaxed circle, (DL) double-strand linear, (SS) single-strand viral DNA. (C) Reduction of HBV precore and pregenomic RNA (3.5 kb) and envelope-specific mRNA (2.4/2.1 kb) was detected by cotransfection with miR-130a expression vector and Northern blot analysis. (D) Reduction of intracellular HBV core protein (HBc) was detected by cotransfection with miR-130a via Western blot analysis. (E) (Upper panel) Potential microRNA target sites on HBV *ayw* genome were predicted by different computer algorithms. (Lower panel) HuH-7 cells were cotransfected with a luciferase reporter plasmid containing HBV nucleotides 1521–2122 and various miRNA expression vectors. MiR-31-5 was included as a positive control (Materials and Methods). (\*\*) $P < 0.05$ .

assay, and miR-130a had no significant effect on the luciferase activity (Fig. 1E, lower panel).

### Reduction of endogenous miR-130a enhanced HBV DNA replication and protein expression

To further elucidate the inhibition of miR-130a on HBV, we engineered a miR-130a sponge plasmid which contains eight copies of miR-130a synthetic target site at the 3' UTR of a DsRed reporter (Fig. 2A, upper panel). This sponge plasmid can efficiently knockdown the endogenous miR-130a in hepatoma cells by stem-loop qPCR (Fig. 2A, lower panel). Cotransfection of this sponge plasmid with HBV genome significantly increased viral DNA replication (Fig. 2B) and protein synthesis (Fig. 2C). Similar results were obtained when the endogenous miR-130a was sequestered by treatment with LNA-miR-130a antagomir (Fig. 2D–F).

### MiR-130a can knockdown HBV RNA indirectly

Since the reporter assay detected no appreciable effect from miR-130a (Fig. 1F), miR-130a probably attenuated HBV replication via an indirect mechanism, rather than by direct binding to HBV specific RNA. We hypothesized that, miR-130a could reduce HBV replication by targeting a third party host factor positively or negatively, which in turn could act on HBV negatively or positively.

To test further this hypothesis, we asked whether such a putative host factor target could be a transcription factor, which can modulate HBV enhancer/promoter activity (Quasdorff and Protzer 2010; Bar-Yishay et al. 2011). We performed an HBV enhancer/promoter reporter assay with or without miR-130a. The results showed that miR-130a indeed reduced the luciferase activity driven by HBV enhancer-II (Fig. 2G). Consistent with the results of Figure 2G,

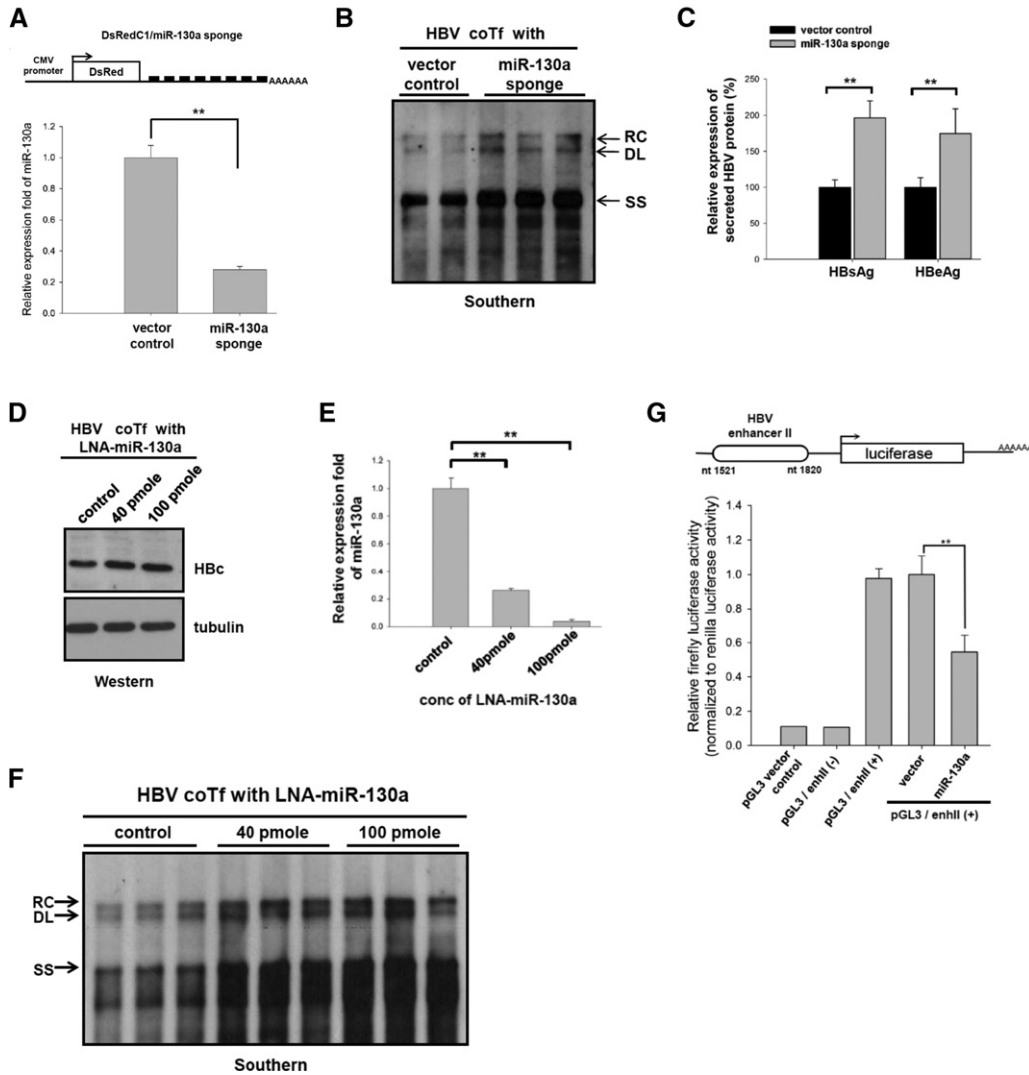


**FIGURE 2.** Reduction of endogenous miR-130a can enhance HBV DNA replication and protein expression. (A) (Upper panel) A cartoon of the miR-130a sponge plasmid. (Lower panel) The reduction of endogenous miR-130a by sponge treatment was measured by stem-loop qPCR. (B) HBV DNA replication was stimulated by the cotransfected miR-130a sponge by Southern blot analysis using an HBV specific probe. The result here is representative of at least three independent experiments. (C) Cotransfection of HBV *ayw* genomic dimer plasmid with miR-130a sponge enhanced levels of secreted HBsAg and HBeAg by ELISA. (D) Cotransfection of an HBV *ayw* genomic dimer plasmid with LNA-miR-130a antagomir increased the intracellular HbC protein level in a dose-dependent manner by Western blot assay. (E) The relative amounts of endogenous miR-130a sequestered at different doses of LNA-miR-130a were measured by stem-loop qPCR. (F) HBV DNA replication was enhanced by LNA-miR-130a treatment which can antagonize and reduce the endogenous miR-130a. HepG2 cells were cotransfected with HBV DNA and LNA-miR-130a or a scramble control at indicated concentrations. The result here is representative of at least three independent experiments. (G) MiR-130a can reduce the activity of HBV enhancer II in HuH-7 cells. HBV enhancer II-containing reporter (pGL3/enhII) was cotransfected with various miRNA expression vectors or vector control (Materials and Methods). pGL3/enhII (-) was a negative control carrying an HBV enhancer II in an anti-sense orientation. (\*\*)  $P < 0.05$ .

we obtained no direct effect of miR-130a on the sequences of HBV pregenomic RNA. When we cotransfected HepG2 cells with a miR-130a expression vector and an HBV replicon plasmid pCHT-9/3091 (a plasmid carrying a 1.3mer HBV *ayw* genome driven by a CMV promoter) (Nassal 1992), we detected no apparent effect of miR-130a on HBV DNA replication (Supplemental Fig. S2, left panel) and protein production (Supplemental Fig. S2, right panel). These results indicate that the negative effect of miR-130a on HBV was not directly mediated through any of the comput-

er-predicted potential binding sites of miR-130a on pgRNA (Fig. 1E).

### MiR-130a directly targets at both PGC1 $\alpha$ and PPAR $\gamma$

To identify such a target transcription factor of miR-130a in hepatocytes, we used four different microRNA target prediction algorithms, and PPARGC1 $\alpha$  (*PGC1 $\alpha$* ) was the only factor whose 3' UTR was consistently predicted by all four programs (Table 2). To experimentally validate the

**TABLE 2.** Prediction of miR-130a target sites at the 3' UTR of human transcription factors known to influence HBV transcription

Transcription factors <sup>a</sup>	Target scan	PicTar	DIANA	RNAhybrid
HNF1	+	-	-	-
HNF4 $\alpha$	+	-	-	-
C/EBP $\alpha$	-	-	-	-
C/EBP $\beta$	-	-	-	-
SP1	+	-	+	-
RXR $\alpha$	+	-	+	-
PPAR $\alpha$	+	-	-	-
PPAR $\gamma$	+	-	-	+
FoxA3 (HNF3 $\gamma$ )	-	-	-	-
FoxO1	-	-	-	-
FXR $\alpha$	-	-	-	-
PGC1 $\alpha$	+	+	+	+
ERR $\alpha$	-	-	-	-
COUP-TF	-	-	-	-
LRH	-	-	-	-

<sup>a</sup>These transcription factors had been reported to be involved in HBV RNA synthesis in literatures (Quasdorff and Protzer 2010). MiR-130a was shown to target at the 3' UTR of PPAR $\gamma$  in adipocytes (Lee et al. 2011).

computer predictions, we established stable cell lines expressing miR-130a (Fig. 3A). While the expression levels of most known hepatic transcription factors remained unchanged in miR-130a expressing cell lines, simultaneous reduction in PPAR $\gamma$  and PGC1 $\alpha$  mRNAs was observed by real-time qPCR analysis (Fig. 3B). To further investigate the effect of miR-130a on PPAR $\gamma$  and PGC1 $\alpha$  expression, we performed Northern and Western blot analyses of PPAR $\gamma$  and PGC1 $\alpha$  in the stable miR-130a expressing cell lines. Concurrent reduction of PPAR $\gamma$  and PGC1 $\alpha$  mRNAs (Fig. 3C) and proteins (Fig. 3D) were observed. It suggests that miR-130a can target both PPAR $\gamma$  and PGC1 $\alpha$ . In a reciprocal experiment, HepG2 cells were treated with LNA-miR-130a antagomir, and significant increase of PGC1 $\alpha$  mRNA and protein was observed (Fig. 3E). Therefore, miR-130a probably reduced PPAR $\gamma$  and PGC1 $\alpha$  protein levels (Fig. 3D) by reducing their respective mRNA levels (Fig. 3C,E). Our result of PPAR $\gamma$  here in hepatocytes is supported by a recent report that miR-130a targets directly the 3' UTR of PPAR $\gamma$  in adipocytes (Lee et al. 2011). To distinguish between a direct and an indirect mechanism of miR-130a on reducing PGC1 $\alpha$  mRNA, we first conducted a reporter assay using a 3' UTR from PGC1 $\alpha$ . The results support for a functional interaction between miR-130a and the 3' UTR of PGC1 $\alpha$  (Supplemental Fig. S3). Next, we introduced mutations into the seed sequences of miR-130a as well as compensatory mutations into its evolutionarily conserved target site of PGC1 $\alpha$  (Fig. 3F). By cotransfection assay, only the combination of a seed mutant miR-130a and a compensatory target mutant PGC1 $\alpha$  could successfully restore the inhibitory effect of miR-130a on the luciferase activity. In a dose-dependent manner, miR-130a could reduce, while LNA-miR-130a could increase, the lucif-

erase activity of a reporter containing the 3' UTR of PGC1 $\alpha$  (Fig. 3G). Taken together, miR-130a can directly target at the 3' UTR of PGC1 $\alpha$ .

### Stimulatory effect of PPAR $\gamma$ and PGC1 $\alpha$ on enhancing HBV DNA replication

We confirmed previous reports (Shlomai et al. 2006; Ondracek et al. 2009) that PGC1 $\alpha$  could stimulate HBV replication by using a siRNA approach (Fig. 4A–D; Supplemental Fig. S4). In order to clarify the role of PGC1 $\alpha$  in the relationship between HBV and miR-130a, we cotransfected different doses of PGC1 $\alpha$  expression vector with constant amount of HBV genomic dimer into stable miR-130a expressing HepG2 cells. Both HBV DNA replication and protein synthesis were gradually increased in a dose-dependent manner (Fig. 4E,F; Supplemental Fig. S5). To date, it remains controversial whether PPAR $\gamma$  (or its agonists) has a positive or negative effect on HBV replication (Yu and Mertz 2001; Wakui et al. 2010; Yoon et al. 2011). By increasing the concentration of a PPAR $\gamma$  agonist (Rosiglitazone), we observed increasing HBV replication (Fig. 5A, left panel). In contrast, when PPAR $\gamma$  antagonist (GW9662) was increased in concentration, both HBV replication and protein expression were significantly reduced (Fig. 5A, right panel). Interestingly, we uncovered here for the first time that the combination of both PPAR $\gamma$  and PGC1 $\alpha$ , in the absence of any exogenous ligands, exhibited a dramatic effect on both HBV DNA replication (Fig. 5B, left panel) and secretions of HBsAg and HBeAg (Fig. 5C, left panel). Conversely, cotransfection of HBV *ayw* genomic dimer with the combination of both PGC1 $\alpha$  and PPAR $\gamma$  siRNAs, resulted in the most potent inhibitory effect on both HBV DNA replication (Fig. 5B, right panel) and secretions of HBsAg and HBeAg (Fig. 5C, right panel).

Finally, we found no apparent change in miR-130a expression in stable PGC1 $\alpha$ -expressing cell lines (Fig. 6A). In contrast to PGC1 $\alpha$ , the expression of miR-130a was reduced in pooled stable PPAR $\gamma$ -expressing cell lines, and could be further reduced by Rosiglitazone, but not by GW9662 treatment (Fig. 6B). We therefore established a triad diagram with a positive feed-forward loop (Fig. 6C). In this triad relationship, miR-130a can indirectly attenuate HBV DNA replication and gene expression by dual targeting at both PPAR $\gamma$  and PGC1 $\alpha$ , which have a stimulatory effect on HBV replication. Because of the feed-forward nature, this loop can presumably amplify a weak signal and convert it into a stronger one.

One important issue to address here is how the expression of miR-130a can be regulated. Bioinformatic analysis revealed three potential binding sites for transcription factors NF- $\kappa$ B/p65, Egr-1, and CREB, at ~1000 nt upstream of the transcription start site (Fig. 7A). We conducted a promoter assay of miR-130a using a luciferase reporter (Fig. 7B). When the binding site of NF- $\kappa$ B/p65 is deleted, luciferase

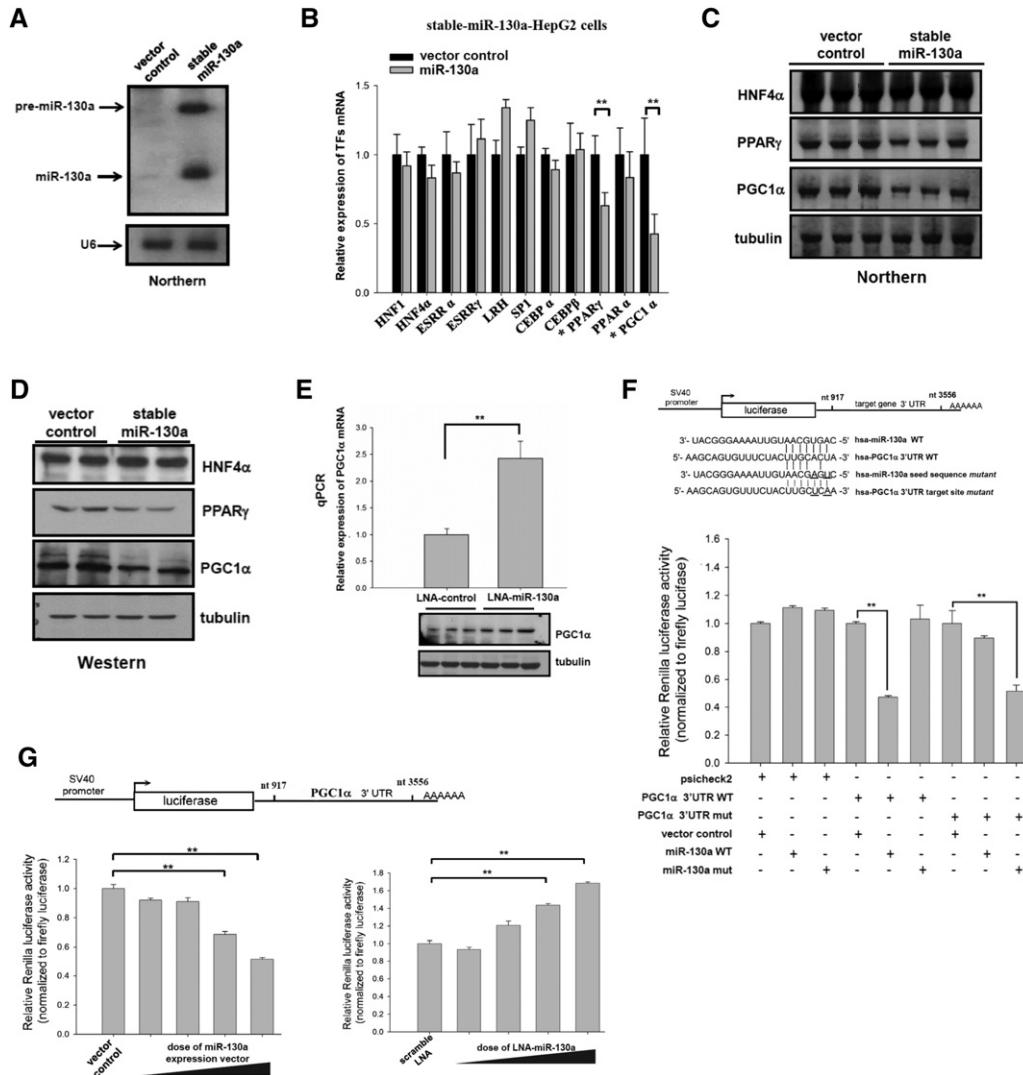


**FIGURE 3.** Identification of host factors targeted by miR-130a. (A) Northern blot analysis of miR-130a precursor and its mature form in HepG2 cell lines stably transfected with a miR-130a expression vector. (B) As implicated by bioinformatic analysis in Table 2, RT-qPCR analysis detected the reduction of PGC1α and PPARγ mRNAs (in asterisk) in stable miR-130a expressing HepG2 cell lines. (C) Northern blot analysis detected concurrent reduction of PGC1α (2.3 kb) and PPARγ (1.4 kb) mRNAs in stable miR-130a expressing cell lines. HNF4α and tubulin were included as a control. (D) Western blot analysis detected concurrent reduction of PGC1α (91 kDa), and PPARγ (54 kDa) proteins in stable miR-130a expressing cells. (E) HepG2 cells were transfected with LNA-miR-130a or a LNA scramble control. The increased PGC1α mRNA and protein levels were measured by real-time RT-qPCR (upper panel) and Western blot analysis (lower panel), respectively. (F) MiR-130a was shown to directly target at the 3' UTR (nucleotides 2025–2031) of PGC1α by compensatory mutagenesis. Mutation sites of the miR-130a seed sequence mutant and the PGC1α target site mutant were underlined in sequence alignment. The reduction of luciferase activity was observed when wild-type miR-130a was in combination with wild-type PGC1α 3' UTR, or when seed mutant miR-130a was in combination with target site mutant of PGC1α. (G) Cotransfection of the PGC1α 3' UTR luciferase reporter with increasing amounts of a miR-130a expression vector resulted in gradually decreasing reporter activity in a dose–response manner (left panel). Conversely, treatment with increasing amounts of a LNA-miR-130a plasmid resulted in gradually increasing reporter activity in a dose–response manner (right panel). (\*\*)*P* < 0.05.

activity is significantly reduced. This result strongly suggests that NF-κB/p65 is a positive activator for miR-130a transcription. Indeed, when a rat or mouse NF-κB/p65 expression vector was cotransfected with the luciferase reporter driven by a miR-130a promoter, a 30–60-fold increase of luciferase activity was observed (Fig. 7C). Consistent with this finding, an siRNA treatment specific for NF-κB/p65 significantly reduced the endogenous level of miR-130a in trans-

fected HepG2 cells by stem–loop qPCR measurement (Fig. 7D). It has been reported that PPARγ can serve as an E3 ligase for NF-κB/p65 ubiquitination and degradation (Ruan et al. 2003; Pascual et al. 2005; Hou et al. 2012). Indeed, we observed significant reduction in the NF-κB/p65 protein level in stable PPARγ-expressing HepG2 cells by Western blot analysis (Fig. 7E, left panel). Interestingly, the NF-κB/p65 protein level was increased significantly in stable miR-130a

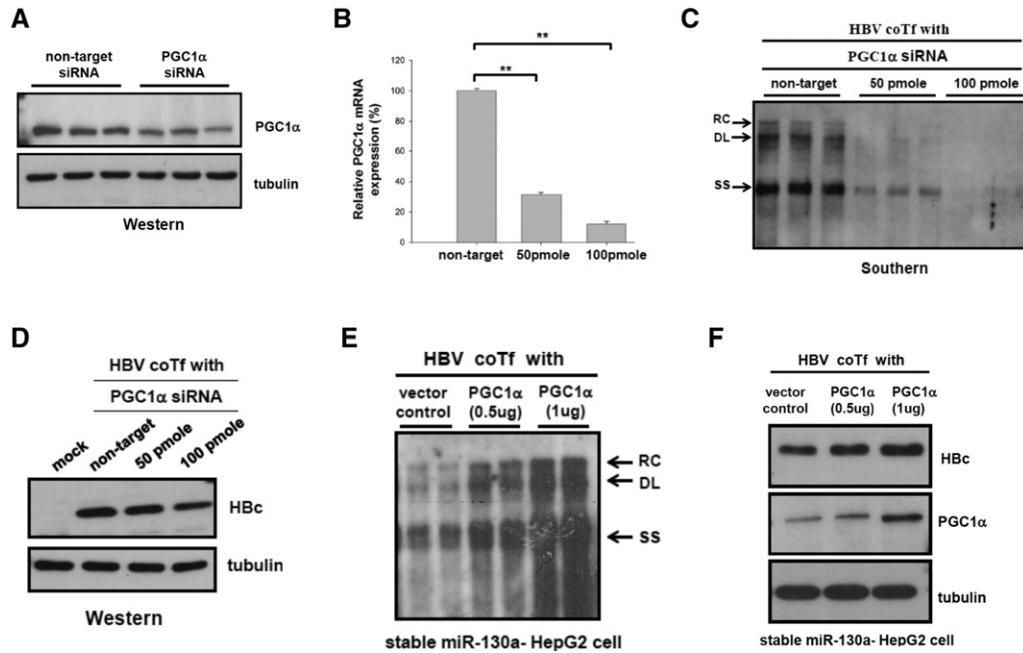


**FIGURE 4.** MiR-130a can attenuate HBV DNA replication and protein expression by targeting at a major metabolic regulator—PGC1 $\alpha$  in hepatocytes. (A–D) HepG2 cells were cotransfected with HBV *ayw* dimer and siRNA-PGC1 $\alpha$  or a nontarget control. Depletion of endogenous PGC1 $\alpha$  by siRNA treatment resulted in repression of HBV DNA replication and protein expression. The efficiency of siRNA treatment for PGC1 $\alpha$  was monitored by Western blotting (A) and real-time RT-qPCR (B). (C) Gradually decreased HBV DNA replication by Southern blot analysis was observed when siRNA concentration was increased. The result here is representative of at least three independent experiments. Reduced intracellular HBC protein was detected by Western blotting using an anti-core antibody (D). (E,F) A stable miR-130a expressing HepG2 cell line was cotransfected with HBV *ayw* dimer and increasing doses of a PGC1 $\alpha$  expression vector. Gradual increases in viral replication by Southern blot analysis (E), as well as intracellular HBC protein by Western blot analysis (F), were observed. This PGC1 $\alpha$  expression vector contains a 3' UTR with no predicted target site for miR-130a, and is considered miR-130a-resistant (Materials and Methods). The dose–response relationship between PGC1 $\alpha$  and viral replication was more apparent, when a derivative of HepG2 recipient cells, stably expressing miR-130a, was used (Materials and Methods).

expressing HepG2 cells (Fig. 7E, right panel). This result is consistent with the fact that miR-130a can target PPAR $\gamma$  (Fig. 3C,D). The negative effect of PPAR $\gamma$  on NF- $\kappa$ B/p65 is not mediated by reducing the mRNA level of NF- $\kappa$ B/p65 by qPCR analysis (Fig. 7F). We also investigated the effect of HBV on the protein level of NF- $\kappa$ B/p65 in HBV-producing cell lines (Fig. 7G). Both phosphorylated and total NF- $\kappa$ B/p65 proteins were significantly reduced in the presence of HBV replication by Western blot analysis. Again, these results are consistent with the negative effect of PPAR $\gamma$  on NF- $\kappa$ B/p65 protein via ubiquitination and degradation (Hou et al. 2012). Finally, when HBV-producing stable cell lines UP7-4 and UP7-7 were treated with siRNA-specific for PPAR $\gamma$ , both NF- $\kappa$ B/p65 and miR-130a were increased (Fig. 7H). Taken together, we postulated here another feed-forward loop between miR-130a and NF- $\kappa$ B/p65 via PPAR $\gamma$  (Fig. 7I). In this context, miR-130a can be considered as an inflammatory microRNA in hepatocytes.

### MiR-130a in hepatic gluconeogenesis and lipogenesis

The dual targets of PGC1 $\alpha$  and PPAR $\gamma$  by miR-130a strongly suggest its important role in energy metabolism. We thus ex-

amined several key metabolic enzymes in glycolysis and gluconeogenesis using stable miR-130a expressing cells. Both phosphoenolpyruvate carboxykinase (PEPCK) and glucose-6-phosphatase (G6Pase) are rate-limiting gluconeogenic enzymes known to be under the positive control of PGC1 $\alpha$  (Yoon et al. 2001). Since both PGC1 $\alpha$  mRNA and proteins were reduced in miR-130a expressing cells (Fig. 3C,D), it was anticipated that PEPCK and G6Pase should be reduced as well. Indeed, concurrent reductions of both PEPCK and G6Pase mRNAs (Fig. 8A) and proteins (Fig. 8B) were observed in miR-130a expressing hepatocytes (designated as miR-130a-HuH-7 or miR-130a-HepG2). While this result suggested a “pro-glycolysis” rather than a “pro-gluconeogenesis” pathway for the role of miR-130a, it would be more certain if key glycolytic enzymes, such as pyruvate kinase (PKLR) and glucokinase (GCK), were not reduced simultaneously. Indeed, the protein expression of GCK and PKLR was not reduced. In fact, PKLR was even increased in miR-130a-HuH-7 cells, while GCK was increased in miR-130a-HepG2 cells (Fig. 8B). Furthermore, we observed increased mRNA expression of both GCK and PKLR in miR-130a expressing HepG2 and HuH-7 cells (Fig. 8C). Consistent with the reduction of miR-130a in HBV-producing UP7-4 and

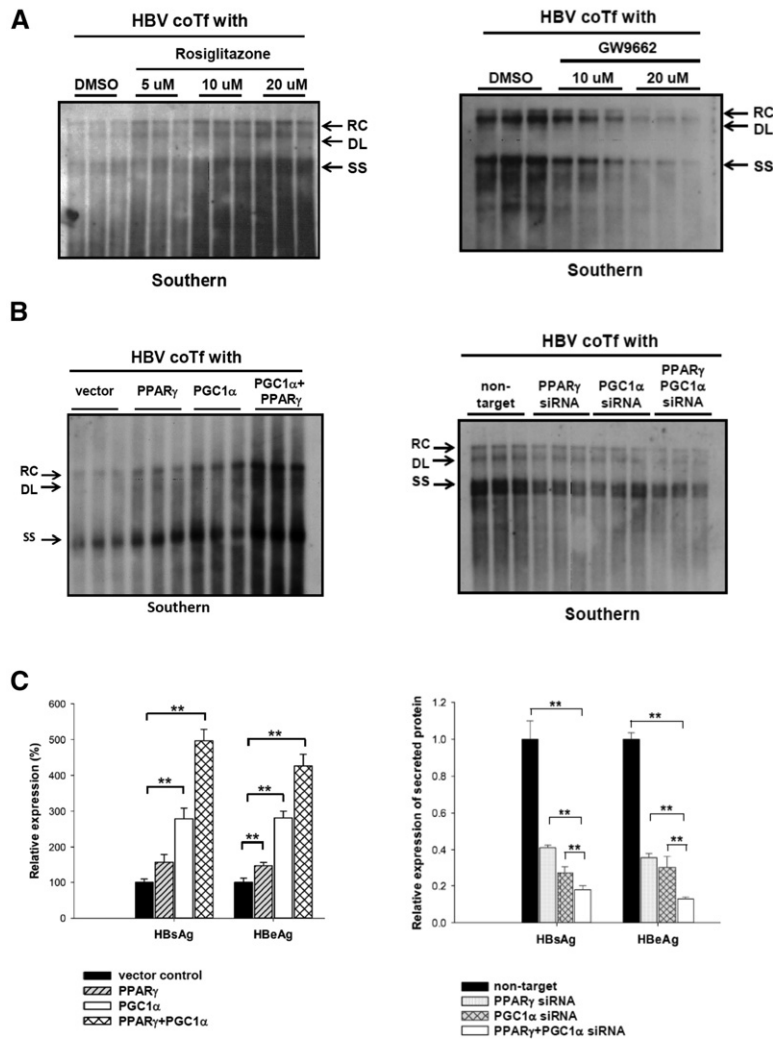


**FIGURE 5.** The combination of PGC1 $\alpha$  and PPAR $\gamma$  can strongly stimulate HBV DNA replication and protein expression. (A) HepG2 cells were transiently transfected with HBV *ayw* dimer and 48 h later, followed by treatment of a PPAR $\gamma$  ligand, Rosiglitazone, at increasing concentrations (Materials and Methods). HBV DNA replication by Southern blot analysis was gradually increased in a dose-dependent manner (left panel). Conversely, when HBV-transfected cells were treated with increasing doses of a PPAR $\gamma$  antagonist, GW9662, it resulted in gradually decreasing replication of HBV DNA (right panel). The result here is representative of at least three independent experiments. (B) Cotransfection of HBV *ayw* dimer with the combination of both PGC1 $\alpha$  and PPAR $\gamma$  expression vectors resulted in further increase in HBV DNA replication (B, left panel) and protein expression of HBsAg and HBeAg (C, left panel). Conversely, cotransfection of HBV *ayw* dimer with the combination of both PGC1 $\alpha$  and PPAR $\gamma$  siRNAs resulted in the most potent inhibitory effect on HBV DNA replication (B, right panel) and expression of HBsAg and HBeAg (C, right panel). HBsAg and HBeAg were detected by ELISA assay. The result here is representative of at least three independent experiments.

UP7-7 cells (Fig. 1A, Table 1), PGC1 $\alpha$ , PEPCK, G6Pase, and PPAR $\gamma$  were all significantly increased (Fig. 8D). One take-home message here is that miR-130a can not only inhibit HBV replication, but also contribute to downregulation of gluconeogenesis and up-regulation of glycolysis in hepatocytes via PGC1 $\alpha$ . In addition to glucose metabolism, we also examined the effect of miR-130a on mitochondria (St-Pierre et al. 2006). By qPCR analysis, we detected reproducible reduction in the mRNA levels of SOD2 (manganese superoxide

dismutase 2) (data not shown). Recently, PPAR $\gamma$  was reported to have a positive effect on the expression of several lipogenic genes (Liu et al. 2012). We therefore examined the potential effect of miR-130a on lipogenic gene expression via PPAR $\gamma$  in stable miR-130a expressing HepG2 cells. We detected significant reduction in the RNA expression of *PPAR $\gamma$*  and *Scd1* (stearoyl CoA desaturase) by qPCR analysis (data not shown).

### HBV transgenic mice exhibited reduced levels of miR-130a

We extended our studies to HBV transgenic mice (Chen et al. 2007), whose liver contain active HBV replication (Fig. 9A). In this animal model, hepatic miR-130a was significantly reduced (Fig. 9B). While the change in total NF- $\kappa$ B/p65 protein was only modest in HBV transgenic mice, the reduction in phosphorylated NF- $\kappa$ B/p65 protein was more apparent (Fig. 9C). Similarly, PGC1 $\alpha$ , G6Pase, PEPCK, PPAR $\gamma$  were all significantly increased in HBV transgenic mice (Fig. 9C). Taken together, it therefore appears that miR-130a is strategically positioned at the intersection of two positive feed-forward loops, linking the metabolic and the immune pathways (Fig. 10A).

### DISCUSSION

We identified a cellular microRNA-130a which can attenuate HBV DNA replication by reducing HBV transcription and protein synthesis (Fig. 10A). Since miR-130a can inhibit the replication of HBV of different genotypes (data not shown), the therapeutic potential of miR-130a may be worth further investigation (Pedersen et al. 2007).

One of the most salient features of miR-130a is in its dual targets at PGC1 $\alpha$  and PPAR $\gamma$  (Fig. 3C–F), leading to reduced HBV replication (Fig. 1B). Conversely, HBV can reduce the expression of miR-130a (Table 1; Fig. 1A), leading to increased expression of PPAR $\gamma$  and PGC1 $\alpha$  (PEPCK and G6Pase) (Fig. 8A,B,D). The level of miR-130a was reduced by overexpression of PPAR $\gamma$ , or by treatment with Rosiglitazone—a PPAR $\gamma$  agonist (Fig. 6B). Taken together, we demonstrated a positive feed-forward loop between HBV, PGC1 $\alpha$  and PPAR $\gamma$ , and miR-130a



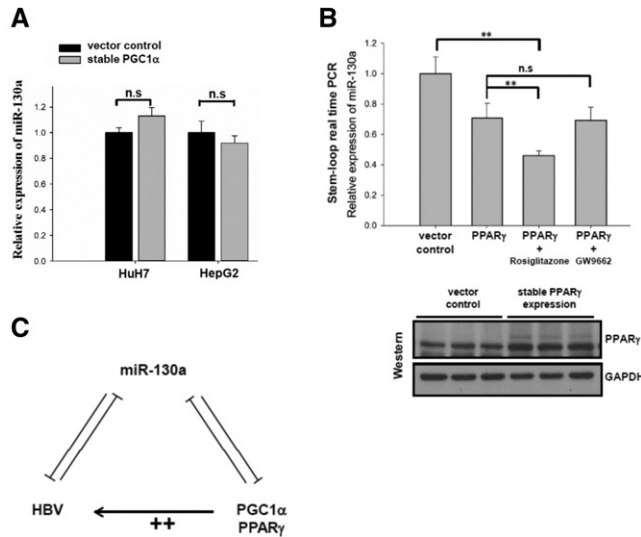


**FIGURE 6.** The effect of PGC1 $\alpha$  and PPAR $\gamma$  on the expression of miR-130a. (A) The expression level of miR-130a was not affected in stable PGC1 $\alpha$ -expressing HepG2 or HuH7 cell lines. (B) (Upper panel) Reduction of miR-130a was observed in PPAR $\gamma$ -expressing HepG2 cell lines using stem-loop qPCR. U6 snRNA was used as an internal control for normalization. Rosiglitazone, but not GW9662, further reduced the expression of miR-130a. (Lower panel) Increased amounts of PPAR $\gamma$  protein in stable PPAR $\gamma$ -expressing HepG2 cell lines were detected by Western blot. (C) This cartoon summarizes the relationships among PPAR $\gamma$ , PGC1 $\alpha$ , miR-130a, and HBV. A feed-forward amplification loop among HBV, PGC1 $\alpha$ , and PPAR $\gamma$  can be mediated through a miR-130a intermediate. The symbol ++ represents an enhanced stimulatory effect from the combination of PGC1 $\alpha$  and PPAR $\gamma$ .

(Fig. 6C). Because HBV replication can be strongly stimulated by the combined effect of PGC1 $\alpha$  and PPAR $\gamma$ , it is possible that HBV could benefit itself by reducing the level of miR-130a during evolution, which targets two major metabolic regulators PGC1 $\alpha$  and PPAR $\gamma$ . The feed-forward loop in Figure 6C could in theory amplify a weak primary signal of miR-130a, PGC1 $\alpha$ , or PPAR $\gamma$ , by going through this loop repetitive rounds. The physiological and pathological significance of miR-130a remains to be further investigated in animal models in the future.

So, how could HBV manipulate the endogenous level of miR-130a in infected hepatocytes? Intriguingly, we identified an NF- $\kappa$ B/p65 binding site in the promoter region of miR-130a (Fig. 7B; Zhou et al. 2010a). NF- $\kappa$ B (p65 and p50) is known to be associated with inflammation (Hayden and Ghosh 2004; Karin 2006). We observed that both endogenous and exogenous NF- $\kappa$ B/p65 could transactivate the promoter of miR-130a (Fig. 7C,D), and the level of miR-130a appeared to be in parallel with that of NF- $\kappa$ B/p65 (Fig. 7E). We speculated that HBV infection, in the absence of an immune system, could reduce the endogenous level of NF- $\kappa$ B/p65, leading to a reduced transcription level of miR-130a. Indeed, in stable HBV-producing cell culture, the total protein level of NF- $\kappa$ B/p65 was significantly reduced (Fig. 7G).

It has been reported that overexpression of HBx alone, in the absence of HBV replication, can activate NF- $\kappa$ B/p65 in hepatoma cells (Su and Schneider 1996; Waris et al. 2001; Slagle et al. 2014). Furthermore, inhibition of HBV replication by TNF- $\alpha$  treatment could involve NF- $\kappa$ B activation (Biermer et al. 2003; Slagle et al. 2014). NF- $\kappa$ B activation by HBx alone (in the absence of HBV replication) could result in cytokine productions of IL-6, IP-10, and IL23 (Lee and Koretzky 1998; Zhou et al. 2010b; Xia et al. 2012). We speculate here that the inhibitory effect of NF- $\kappa$ B on HBV could be mediated in part via miR-130a. In contrast to HBx, either HBV polymerase (in the context of HBV replication) or HBeAg (in the absence of HBV replication), was shown to suppress NF- $\kappa$ B signaling (Wang and Ryu 2010; Wilson et al. 2011; Liu et al. 2014). Our results of Figure 7G using the HBV replication system in cell culture are consistent with the suppression of NF- $\kappa$ B by HBV polymerase or HBeAg.

In literature, PGC1 $\alpha$  has also been associated with suppression of inflammation (Tran et al. 2011; Eisele et al. 2013; Qian et al. 2013). It was shown that PGC1 $\alpha$  protein can inhibit the activation and phosphorylation of NF- $\kappa$ B, without altering the total protein level of NF- $\kappa$ B (Eisele et al. 2013). This relationship between NF- $\kappa$ B and PGC1 $\alpha$  could explain why the level of phosphorylated NF- $\kappa$ B protein was reduced in HBV transgenic mice, yet, the level of total NF- $\kappa$ B protein remained more or less the same (Fig. 9C). Taken together, it is conceivable that during hepatic inflammation (hepatitis), NF- $\kappa$ B/p65 could be activated (Hayden and Ghosh 2004; Karin 2006), leading to an elevated level of miR-130a (Fig. 10A), which in turn could reduce HBV replication and contribute to viral clearance (Fig. 10B, left panel). In contrast, in many healthy (asymptomatic) HBV carriers, persistent HBV replication can reduce miR-130a, promote PGC1 $\alpha$  and PPAR $\gamma$ , suppress NF- $\kappa$ B, and thus contribute to dampened inflammation and failure of viral clearance (Fig. 10B, right panel). It remains to be further investigated in the future whether miR-130a could be involved in cytotoxic T lymphocytes (CTL) or cytokine-mediated liver inflammation and viral clearance (Bertoletti et al. 1991; Guidotti et al. 1994; Chisari and Ferrari 1995).

We noted that there are recent reports about the effect of miR-130a on the immune response in HCV-infected hepatocytes (Bhanja Chowdhury et al. 2012; Zhang et al. 2013). Again, NF- $\kappa$ B/p65 should be elevated in liver inflammation in hepatitis C, which could lead to an elevated level of miR-130a in HCV-infected hepatocytes. It will be interesting to extend our current study of miR-130a/PGC1- $\alpha$  from HBV- to HCV-infected liver in the future. For example, this hypothesis of miR-130a/PGC1- $\alpha$  could be tested experimentally by comparing the hepatic levels of miR-130a, PGC1 $\alpha$  and PPAR $\gamma$ , and viral titers of HBV or HCV, before, during and after acute exacerbation in chronic hepatitis B or C patients.

It has been well documented that chronic HCV infection is associated with a higher incidence of type 2 diabetes

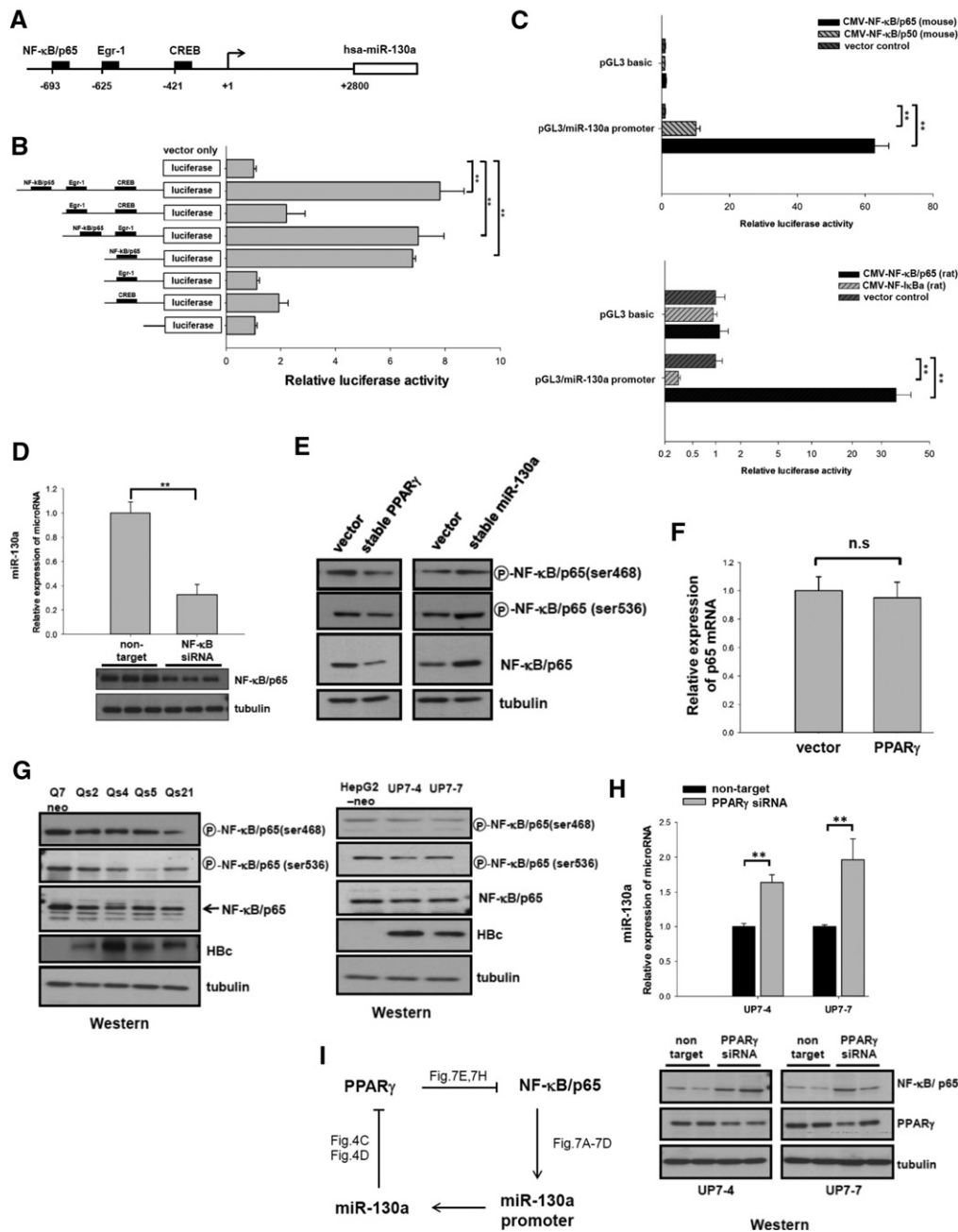


**FIGURE 7.** A feed-forward loop between NF-κB/p65 and miR-130a via PPAR $\gamma$ . The promoter activity of miR-130a can be stimulated by NF-κB/p65, while PPAR $\gamma$  appeared to reduce the protein level of NF-κB/p65. (A) A schematic diagram shows several potential binding sites for transcription factors in the putative hsa-miR-130a promoter element upstream of the transcription start site (+1): A putative NF-κB/p65 binding site at -693 position was as previously reported (Zhou et al. 2010a), and the sites at -625 and -421 for Egr-1 and CREB were predicted using the online softwares Promo and TRANSFAC (Wingender et al. 2000; Messeguer et al. 2002). (B) Analysis of miR-130a promoter by deletion mapping and reporter assay. Briefly, HuH-7 cells were transfected with various luciferase reporter constructs containing sequentially deleted hsa-miR-130a promoter. Deletion of an NF-κB/p65 binding site resulted in significantly reduced reporter activity. (C) (Upper panel) Both NF-κB/p65 and p50 can stimulate miR-130a promoter activities by ~60-fold and 10-fold, respectively. HuH-7 cells were cotransfected with expression vectors of either pCMV-mouse NF-κB/p65 or p50, and a luciferase reporter driven by an hsa-miR-130a promoter. (Lower panel) A 30-fold stimulation effect on miR-130a promoter was obtained by using a rat pCMV-flag- NF-κB/p65. Cotransfection with a rat IκB expression vector repressed the luciferase activity by about fourfold. Relative luciferase values for each transfection were normalized with cotransfected renilla expression. (D) Conversely, knockdown of the endogenous NF-κB/p65 by siRNA resulted in decreased expression of miR-130a by stem-loop qPCR analysis. (E) (Left panel) A PPAR $\gamma$  stable expression cell line of HepG2 origin exhibited reduced levels of phosphorylated and total NF-κB/p65 protein by Western blot analysis. (Right panel) In contrast, a miR-130a stable expression cell line exhibited increased levels of phosphorylated and total NF-κB/p65 protein. (F) The relative mRNA level of NF-κB/p65 was not affected in stable PPAR $\gamma$  expressing HepG2 cells by qPCR. (G) The reduction of phosphorylated and total NF-κB/p65 protein was observed in stable HBV-producing rat (left panel) or human (right panel) hepatoma cells by Western blot analysis. (H) Knockdown of the endogenous PPAR $\gamma$  by siRNA treatment was conducted in stable HBV-producing human hepatoma cells UP7-4 and UP7-7. This experiment resulted in increased expression of miR-130a by stem-loop qPCR and NF-κB protein production by Western blot analysis (lower panel). (I) A cartoon summarizes a positive feed-forward loop between miR-130a and NF-κB/p65 via PPAR $\gamma$ . (\*\*)  $P < 0.05$ .

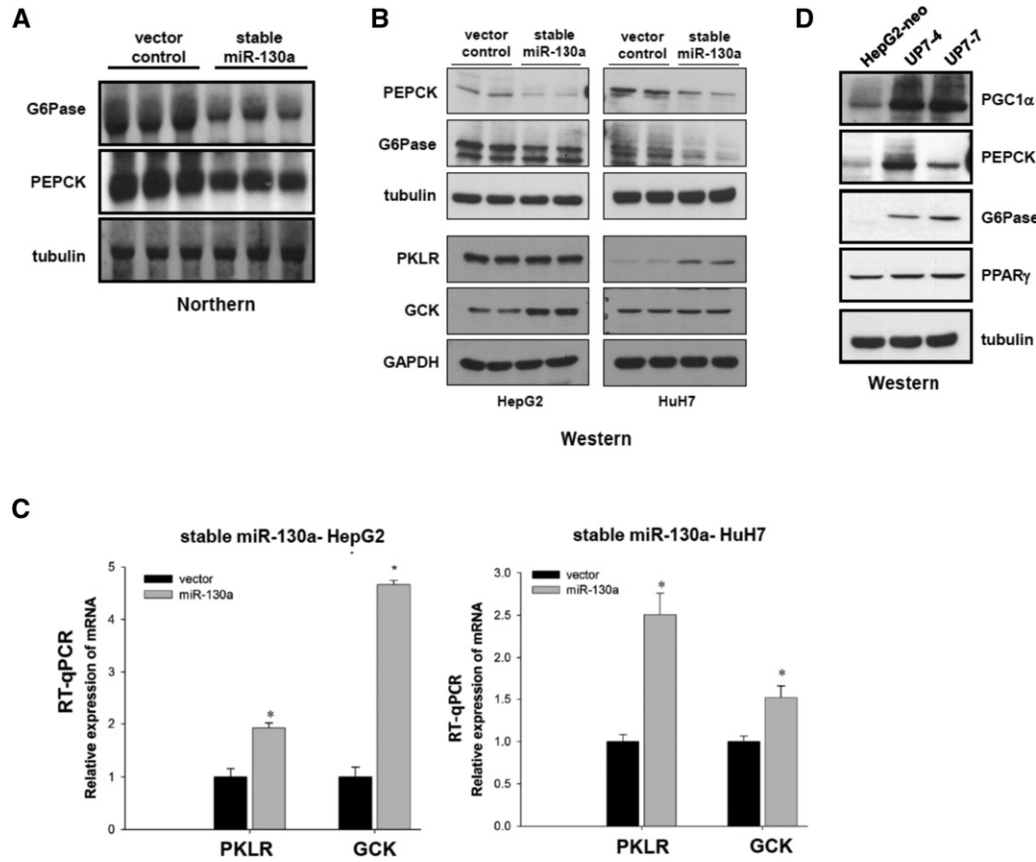


**FIGURE 8.** MiR-130a could play a regulatory role in energy metabolism in hepatocytes. (A) The mRNA expression of G6Pase (1.0 kb) and PEPCK (1.8 kb) was reduced in stable miR-130a expressing HepG2 cells by Northern blot analysis. (B) Reduced protein expression of PEPCK (69 kDa) and G6Pase (40 kDa) was also detected by Western blot analysis. We noted an increased level of glucokinase (GCK) (52 kDa) in stable miR-130a expressing HepG2 cells, and an increased level of pyruvate kinase (PKLR) (58 kDa) in stable miR-130a expressing HuH-7 cells. (C) The levels of PKLR and GCK specific mRNAs were increased in stable miR-130a expressing cells by RT-qPCR analysis. (D) The protein expression of PGC1 $\alpha$  and gluconeogenic enzymes PEPCK and G6Pase in HBV-producing HepG2 cells (UP7-4 and UP7-7) was increased by Western blot analysis.

mellitus (T2DM) (Mason et al. 1999; Mehta et al. 2000). However, unlike HCV, chronic hepatitis B patients do not have higher prevalence of T2DM (Mehta et al. 2000; Huang et al. 2010). In the presence of HBV, miR-130a level was reduced (Table 1; Figs. 1A, 9B), leading to increased PGC1 $\alpha$ , PEPCK, G6Pase, and gluconeogenesis in HBV transgenic mice (Figs. 9C, 10A). On the other hand, reduced amount of miR-130a in HBV-producing hepatocytes can also promote the expression of PPAR $\gamma$  (Fig. 8D), which favors lipogenesis and production of adiponectin. The simultaneous increase of gluconeogenesis and lipogenesis caused by the reduction of miR-130a in HBV-infected hepatocytes could play an important role in liver homeostasis.

As a PPAR $\gamma$  agonist, Rosiglitazone is an option for treatment of T2DM (Cho and Momose 2008). Although no apparent correlation between T2DM and chronic hepatitis B was noted, it is not uncommon that many HBV carriers are also T2DM patients, and *vice versa*. Our result in Figure 5A demonstrated that Rosiglitazone at 10–20  $\mu$ M could strongly stimulate HBV DNA replication in cell culture (Yu and Mertz

2001; Yoon et al. 2011). It therefore cannot be excluded without further clinical studies that an overdosed treatment with Rosiglitazone could risk an episode of viral reactivation in HBV carriers with T2DM. Similarly, endogenous PGC1 $\alpha$  can be elevated in fasting mice (Yoon et al. 2001). If this phenomenon can be extended to humans infected with HBV, it may be a safety practice for HBV carriers to eat their meals at regular hours.

In this study, we relied heavily on the use of in vitro and in vivo transfection systems for our investigation. It would be interesting to further our studies by using the in vitro infection of HepARG or NTCP-HepG2 cell lines (Gripon et al. 2002; Yan et al. 2012). At present, because the infection efficiency remains to be low, the great majority of hepatocytes in culture would remain uninfected, resulting in little changes in the level of miR-130a.

In summary, it is tempting to speculate that HBV could have evolved a strategy to down-regulate the expression of miR-130a and NF- $\kappa$ B, and thus create a niche with more abundant PGC1 $\alpha$  and PPAR $\gamma$ , as well as reduced immune response and inflammation.

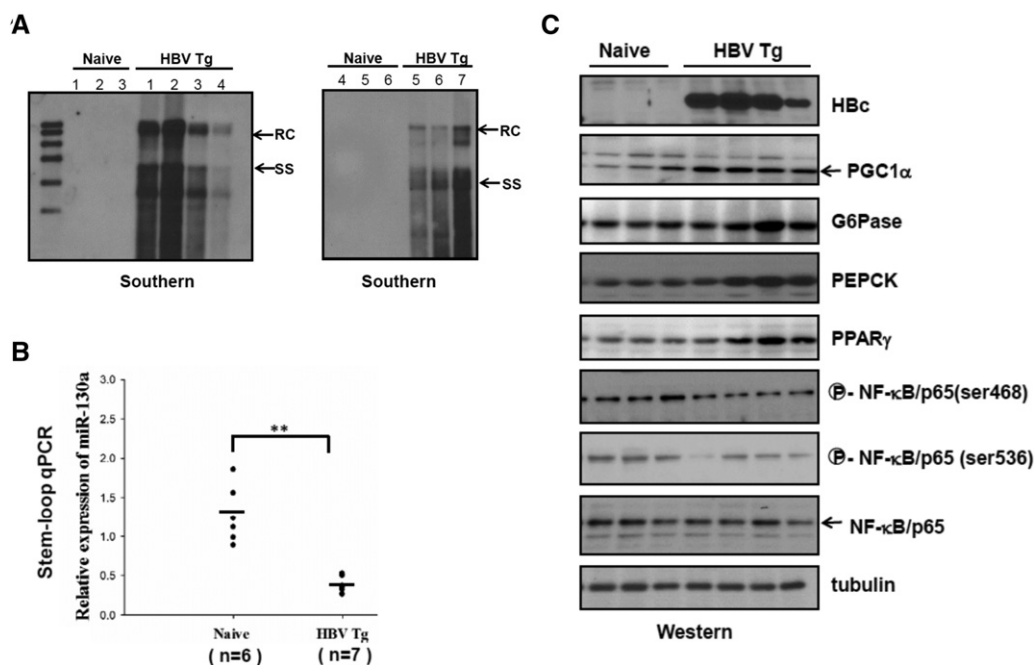


**FIGURE 9.** Metabolic profiles and miR-130a expression in HBV transgenic mice. (A) HBV DNA replication was detected in the liver of HBV transgenic mice by Southern. Samples in each lane are from each individual mouse. The result here is representative of at least three independent experiments. (B) Reduced expression of miR-130a in HBV transgenic mice was compared with that of the parental control mice by stem-loop qPCR analysis. (C) Relative to the wild-type control mice (naive), HBV transgenic mice exhibited decreased expression of NF- $\kappa$ B/p65 and increased expression of HBV core protein, PGC1 $\alpha$ , PEPCK, G6Pase, PPAR $\gamma$ .

## MATERIALS AND METHODS

### Ethics statement

All animal experiments were conducted under protocols approved by Academia Sinica Institutional Animal Care and Utilization Committee (ASIACUC permit number 12-02-322). Research was conducted in compliance with the principles stated in the Guide for the Care and Use of Laboratory Animals, National Research Council, 1996.

### Animals

The generation of HBV transgenic mice on an ICR background has been reported previously (Chen et al. 2007). The transgene is a 1.3-fold HBV genome (genotype D, serotype *ayw*). The Tg [HBV1.3] mouse line was used in this study. All animals were housed in a specific-pathogen-free environment in the animal facility of the Institute of Biomedical Sciences, Academia Sinica.

### Construction of miRNA plasmids

The sequences of human miRNAs were retrieved from Ensembl database and miRBase (Version 16). The primer sequences used in cloning the full-length precursor miRNAs are listed in Supplemental Table S1. The methods to construct the miRNA expression vectors are as detailed elsewhere (Chen et al. 2012). PCR products were subcloned from TA cloning vector (RBC, Taiwan) to pSuper (Oligo-Engine, Inc., Seattle, Washington) by Hind III digestion. All plasmids were confirmed by sequencing. Approximately eight- to 400-

fold higher level of microRNA expression was detected by transfection and stem-loop RT-PCR analysis. MiR-31 was used as a negative control since it had no effect on HBV replication. In contrast, miR-31-5 served as a positive control of an anti-HBV miRNA. MiR-31-5 was constructed from the backbone of miR-31 by reengineering its seed sequences, which are now complementary to nucleotides 1575–1595 of HBV *ayw* genome (GenBank J02203) (Fig. 1E; Ely et al. 2009). The PPAR $\gamma$  and PGC1 $\alpha$  expression vectors were from GeneCopoeia. Plasmids pCMV-SPORT-mouse p50/NF- $\kappa$ B and pCMV-SPORT-mouse p65/NF- $\kappa$ B were kindly provided by Ruey-Bing Ray Yang (Fuchs et al. 2012), and pCMV-Flag-rat I $\kappa$ B $\alpha$  and pCMV-Flag-rat p65/NF- $\kappa$ B were kindly provided by Eminy H.Y. Lee (Tai et al. 2009) (Institute of Biomedical Sciences, Academia Sinica).

### Source of antibodies

anti-HBc (Dako), anti-PPAR $\gamma$  (Santa Cruz Biotechnology), anti-GAPDH, anti-PKLR, anti-G6Pase, anti-tubulin, anti-NF- $\kappa$ B/p65 (GeneTex), anti-PGC1 $\alpha$  (Origene), anti-PCK1 (Abnova), anti-GCK (Biovision), anti-phospho-NF- $\kappa$ B/p65(Ser468), phospho-NF- $\kappa$ B/p65(Ser536) (Cell Signaling Technology, Inc.). Secondary antibodies include mouse anti-rabbit-HRP, goat anti-mouse-HRP (GeneTex), and donkey anti-goat-HRP (Santa Cruz Biotechnology).

### MiR-130a sponge

Each sense and anti-sense oligos (Supplemental Table) were designed to contain four copies of synthetic target sites of miR-130a.

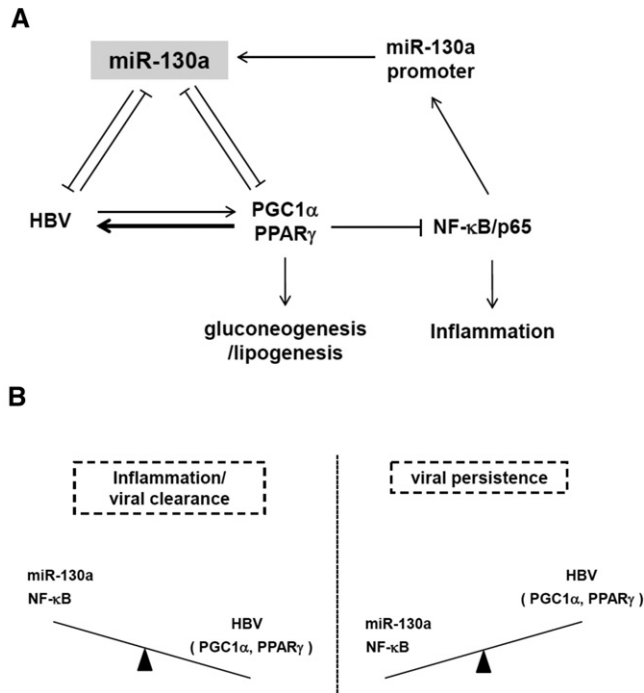


**FIGURE 10.** Diagrams of virus-host interactions between HBV and miR-130a, NF- $\kappa$ B, PGC1 $\alpha$ , and PPAR $\gamma$ . (A) A cartoon summarizes the integration of two positive feed-forward loops from Figures 7I and 6C. In the presence of HBV, the level of miR-130a was reduced (Table 1; Fig. 1A), probably due to a reduced level of NF- $\kappa$ B/p65 in hepatocytes (Figs. 7G, 9C). Since miR-130a can target both PGC1 $\alpha$  and PPAR $\gamma$  mRNAs simultaneously (Figs. 3C,D, 6C), the reduction of miR-130a can result in elevated levels of PGC1 $\alpha$  and PPAR $\gamma$ , which can coactivate HBV transcription, leading to increased HBV DNA replication (Fig. 5B). It has been reported previously that PPAR $\gamma$  protein can serve as an E3 ligase for NF- $\kappa$ B/p65, resulting in NF- $\kappa$ B/p65 protein ubiquitination and degradation, leading to the reduction of NF- $\kappa$ B/p65 and miR-130a promoter activity (Fig. 7I). In this scheme (A), HBV can create a more friendly niche for itself by reducing the level of miR-130a via a positive feed-forward loop (Fig. 7I). Metabolically, PGC1 $\alpha$  is known to be a positive transcriptional coactivator of hepatic gluconeogenesis (Yoon et al. 2001). PPAR $\gamma$  is a positive transcription factor for lipogenesis which in turn can reduce blood glucose level (Yu et al. 2003; Liu et al. 2012). By dual targeting at PGC1 $\alpha$  and PPAR $\gamma$ , miR-130a could play a critical role in glucose homeostasis. (B) Liver inflammation could favor viral clearance, since when NF- $\kappa$ B and miR-130a are elevated, PGC1 $\alpha$ , PPAR $\gamma$ , and HBV replication are reduced. In contrast, when liver is without inflammation, the levels of both NF- $\kappa$ B and miR-130a are low, and the levels of PGC1 $\alpha$  and PPAR $\gamma$  are higher, resulting in more active viral replication.

Annealed oligo product was gel purified before PCR amplification. Gel-purified PCR product was subcloned into DsRedC1 vector at HindIII site. Colonies were screened by PCR and the orientation of the insert and the copy numbers of target sites were confirmed by sequencing.

## Cell culture

Human hepatoma HuH-7 (Nakabayashi et al. 1982), HepG2 (Aden et al. 1979), and rat hepatoma cell line Q7 (Shih et al. 1989) cells were maintained as described previously (Le Pogam et al. 2005; Chua et al. 2010). In general, the phenotype of viral replication

and the effect of microRNA are stronger in HepG2 than HuH-7 cells. However, HuH-7 cells are easier to passage and transfect. Therefore, we used these two cell lines interchangeably.

## PPAR $\gamma$ agonist and antagonist

Rosiglitazone and GW9662 were from Sigma. HepG2 cells were seeded in 6-well tissue culture plates at  $5 \times 10^5$  cells/well. At 48 h post-transfection, Rosiglitazone or GW9662 in 0.1% DMSO was added to medium. Culture medium was changed every 2 d before harvest.

## Quantitative real-time PCR

Briefly, 2  $\mu$ g of total RNA was reverse transcribed into cDNA using random primers and High Capacity cDNA Reverse Transcription kit (Applied Biosystems) at 37°C for 120 min. The cDNA product was analyzed by 1.5% agarose gel electrophoresis staining with HealthView. The cDNA product was then diluted 100 times for real-time PCR analysis using Power SYBR Green PCR master mix (Applied Biosystems), and the default condition in a 20  $\mu$ L reaction volume by Applied Biosystems 7500 Real-Time PCR System. Data were analyzed by relative quantification methods ( $\Delta\Delta$ Ct methods) using 7500 software V2.0.1.

## Stem-loop qPCR for miRNA

Taqman RT and stem-loop real-time assay were from Applied Biosystems: miR-31 (assayID: 002279), miR-130a (assayID: 000454). Briefly, 100 ng RNAs were reverse transcribed by specific stem-loop primer and further analyzed by Taqman real-time PCR assay using default setting. U6 snRNA (assayID: 001973) was used as an internal loading control. Data were analyzed by Applied Biosystems 7500 software V2.0.1.

## Southern and Northern blot

HBV core particle-associated DNA, total cellular cytoplasmic RNA, and microRNA were analyzed by Southern blot and Northern blot as described previously (Le Pogam et al. 2005; Chua et al. 2010).

## MiR-130a promoter analysis by deletion mapping

An upstream fragment of the miR-130a precursor (−750 to −1 nt), containing putative binding sites for NF- $\kappa$ B/p65, Egr-1, and CREB, was amplified by PCR from human HepG2 genomic DNA (Fig. 7B). PCR primers were as listed in Supplemental file. The PCR products were separated by agarose gel electrophoresis, and the isolated DNA fragments were then cloned into the restriction enzyme digested pGL3 Basic Vector (Promega) containing a firefly luciferase reporter (New England Biolabs). Various promoter deletion plasmids, containing shorter fragments upstream of the miR-130a precursor, were derived from the full-length promoter plasmid by PCR amplification and cloning using various PCR primers (Supplemental Table). All the promoter plasmids were confirmed by DNA sequencing. HuH-7 cells were transfected with promoter deletion plasmids for 48 h and firefly luciferase activities were then measured and normalized to each cotransfected renilla luciferase level. The full-length 3' UTRs of PPAR $\gamma$ , PGC1 $\alpha$ , and SP1 were amplified

from genomic DNA of HepG2 cells using their respective forward and reverse primers (Supplemental Table), and cloned into a psiCHECK-2 luciferase vector (Promega). Target site mutants containing altered sequences at PGC1 $\alpha$  3' UTR and a miR-130a mutant containing altered seed sequences, were engineered by using paired mutant primers (Supplemental Table) and Site-directed Mutagenesis kit (Stratagene).

### Stable miR-130a expressing cell lines

Approximately one million HepG2 cells were transiently transfected by 3  $\mu$ g plasmid DNA (pSuper and pSuper-miR-130a) with Polyjet (SigmaGen), followed by G418 selection for 3 wk. The G418-resistant colonies were pooled together.

### LNA-miR-130a knockdown

HepG2 and HuH-7 cells were cotransfected with puromycin resistant plasmid (pTRE2pur) and LNA-scramble control or LNA anti-miR-130a (Locked Nucleic Acid, Exiqon), using Lipofectamine 2000 (Invitrogen). Twelve hours post-transfection, transfected culture was treated with puromycin (2  $\mu$ g/mL) for 2 d, followed by reduced concentration of puromycin (0.5  $\mu$ g/mL) for another 2 d before harvesting for Western blot analysis (Chen et al. 2012).

### Bioinformatic analysis

Computer-based programs including Targetscan (<http://www.targetscan.org/>), Pictar (<http://pictar.mdc-berlin.de/>), Microinspector (<http://bioinfo.uni-plovdiv.bg/microinspector/>), RNAhybrid (<http://www.bibiserv.techfak.uni-bielefeld.de/>), and DIANA (<http://diana.cslab.ece.ntua.gr>) were used to predict potential targets for miR-130a. The minimal free energy of binding  $<-20$  kcal/mol was used as the cut-off value.

### MicroRNA Taqman low density array analysis

The total RNA of HBV-producing cells were extracted by TRIzol (Invitrogen). The quality and quantity of RNA samples were determined by Agilent 2100 Bioanalyzer using RNA 6000 Nano Kit (Agilent Technologies, Inc.). The reverse transcription reactions were performed using TaqMan MicroRNA Reverse Transcription kit (Applied Biosystems). The expression of miRNA was detected by TaqMan Rodent MicroRNA Array A (Applied Biosystems), and analyzed by Applied Biosystems 7900 HT Fast Real-Time PCR System containing 381 rodent miRNA targets.

### Bioinformatic analysis of NF- $\kappa$ B/p65 promoter

Analyses of the miR-130a promoter for potential transcription factor binding sites were performed using the online prediction software tools PROMO and TRANSFAC version 8.3 (BioBase Co.).

### Statistics

Statistical significance was determined using the Student's *t*-test. In all figures, values were expressed as mean  $\pm$  standard deviation

(SD) and statistical significance ( $P < 0.05$ ) was indicated by an asterisk. The data represent results from at least three independent experiments.

### SUPPLEMENTAL MATERIAL

Supplemental material is available for this article.

### ACKNOWLEDGMENTS

We thank the technical support from the Affymetrix Gene Expression Service Lab (<http://ipmb.sinica.edu.tw/affy/>), Academia Sinica, Taiwan. We also thank the High Throughput Genomics Core of the Biodiversity Research Center at Academia Sinica for performing the NGS experiments. We are grateful to Dr. Ruey-Bing Yang for plasmids pCMV-SPORT-mouse NF- $\kappa$ B/p50 and pCMV-SPORT-mouse NF- $\kappa$ B/p65, and Dr. Eminy H.Y. Lee for plasmids pCMV-Flag-rat I $\kappa$ B $\alpha$  and pCMV-Flag-rat NF- $\kappa$ B/p65. This work was supported by Ministry of Science and Technology (MOST), Academia Sinica, and National Health Research Institute (NHRI), Taiwan (NHRI-EX99-9903BI and NHRI-EX103-10203BI).

Received October 25, 2014; accepted December 8, 2014.

### REFERENCES

- Aden DP, Fogel A, Plotkin S, Damjanov I, Knowles BB. 1979. Controlled synthesis of HBsAg in a differentiated human liver carcinoma-derived cell line. *Nature* **282**: 615–616.
- Ambros V. 2011. MicroRNAs and developmental timing. *Curr Opin Genet Dev* **21**: 511–517.
- Bar-Yishay I, Shaul Y, Shlomai A. 2011. Hepatocyte metabolic signalling pathways and regulation of hepatitis B virus expression. *Liver Int* **31**: 282–290.
- Bertoletti A, Ferrari C, Fiaccadori F, Penna A, Margolskee R, Schlicht HJ, Fowler P, Guilhot S, Chisari FV. 1991. HLA class I-restricted human cytotoxic T cells recognize endogenously synthesized hepatitis B virus nucleocapsid antigen. *Proc Natl Acad Sci* **88**: 10445–10449.
- Bhanja Chowdhury J, Shrivastava S, Steele R, Di Bisceglie AM, Ray R, Ray RB. 2012. Hepatitis C virus infection modulates expression of interferon stimulatory gene IFITM1 by upregulating miR-130A. *J Virol* **86**: 10221–10225.
- Biermer M, Puro R, Schneider RJ. 2003. Tumor necrosis factor  $\alpha$  inhibition of hepatitis B virus replication involves disruption of capsid integrity through activation of NF- $\kappa$ B. *J Virol* **77**: 4033–4042.
- Chen CC, Ko TM, Ma HI, Wu HL, Xiao X, Li J, Chang CM, Wu PY, Chen CH, Han JM, et al. 2007. Long-term inhibition of hepatitis B virus in transgenic mice by double-stranded adeno-associated virus 8-delivered short hairpin RNA. *Gene Ther* **14**: 11–19.
- Chen HL, Huang JY, Chen CM, Chu TH, Shih C. 2012. MicroRNA-22 can reduce parathyroid hormone expression in transdifferentiated hepatocytes. *PLoS One* **7**: e34116.
- Chisari FV, Ferrari C. 1995. Hepatitis B virus immunopathogenesis. *Annu Rev Immunol* **13**: 29–60.
- Cho N, Momose Y. 2008. Peroxisome proliferator-activated receptor  $\gamma$  agonists as insulin sensitizers: from the discovery to recent progress. *Curr Top Med Chem* **8**: 1483–1507.
- Chua PK, Tang FM, Huang JY, Suen CS, Shih C. 2010. Testing the balanced electrostatic interaction hypothesis of hepatitis B virus DNA synthesis by using an in vivo charge rebalance approach. *J Virol* **84**: 2340–2351.
- Dumortier O, Hinault C, Van Obberghen E. 2013. MicroRNAs and metabolism crosstalk in energy homeostasis. *Cell Metab* **18**: 312–324.

- Eisele PS, Salatino S, Sobek J, Hottiger MO, Handschin C. 2013. The peroxisome proliferator-activated receptor  $\gamma$  coactivator 1 $\alpha/\beta$  (PGC-1) coactivators repress the transcriptional activity of NF- $\kappa$ B in skeletal muscle cells. *J Biol Chem* **288**: 2246–2260.
- Ely A, Naidoo T, Arbuthnot P. 2009. Efficient silencing of gene expression with modular trimeric Pol II expression cassettes comprising microRNA shuttles. *Nucleic Acids Res* **37**: e91.
- Finck BN, Kelly DP. 2006. PGC-1 coactivators: Inducible regulators of energy metabolism in health and disease. *J Clin Invest* **116**: 615–622.
- Fuchs Y, Brunwasser M, Haif S, Haddad J, Shneyer B, Goldshmidt-Tran O, Korsensky L, Abed M, Zisman-Rozen S, Koren L, et al. 2012. Sef is an inhibitor of proinflammatory cytokine signaling, acting by cytoplasmic sequestration of NF- $\kappa$ B. *Dev Cell* **23**: 611–623.
- Galibert F, Mandart E, Fitoussi F, Tiollais P, Charnay P. 1979. Nucleotide sequence of the hepatitis B virus genome (subtype ayw) cloned in *E. coli*. *Nature* **281**: 646–650.
- Gripon P, Rumin S, Urban S, Le Seyec J, Glaize D, Cannie I, Guyomard C, Lucas J, Trepo C, Guguen-Guillouzo C. 2002. Infection of a human hepatoma cell line by hepatitis B virus. *Proc Natl Acad Sci* **99**: 15655–15660.
- Guidotti LG, Ando K, Hobbs MV, Ishikawa T, Runkel L, Schreiber RD, Chisari FV. 1994. Cytotoxic T lymphocytes inhibit hepatitis B virus gene expression by a noncytolytic mechanism in transgenic mice. *Proc Natl Acad Sci* **91**: 3764–3768.
- Hayden MS, Ghosh S. 2004. Signaling to NF- $\kappa$ B. *Genes Dev* **18**: 2195–2224.
- Hou Y, Moreau F, Chadee K. 2012. PPAR $\gamma$  is an E3 ligase that induces the degradation of NF $\kappa$ B/p65. *Nature Commun* **3**: 1300.
- Houten SM, Auwerx J. 2004. PGC-1 $\alpha$ : Turbocharging mitochondria. *Cell* **119**: 5–7.
- Huang ZS, Huang TS, Wu TH, Chen MF, Hsu CS, Kao JH. 2010. Asymptomatic chronic hepatitis B virus infection does not increase the risk of diabetes mellitus: A ten-year observation. *J Gastroenterol Hepatol* **25**: 1420–1425.
- Karin M. 2006. Nuclear factor- $\kappa$ B in cancer development and progression. *Nature* **441**: 431–436.
- Le Pogam S, Chua PK, Newman M, Shih C. 2005. Exposure of RNA templates and encapsidation of spliced viral RNA are influenced by the arginine-rich domain of human hepatitis B virus core antigen (HBcAg 165–173). *J Virol* **79**: 1871–1887.
- Lee JR, Koretzky GA. 1998. Production of reactive oxygen intermediates following CD40 ligation correlates with c-Jun N-terminal kinase activation and IL-6 secretion in murine B lymphocytes. *Eur J Immunol* **28**: 4188–4197.
- Lee EK, Lee MJ, Abdelmohsen K, Kim W, Kim MM, Srikantan S, Martindale JL, Hutchison ER, Kim HH, Marasa BS, et al. 2011. miR-130 suppresses adipogenesis by inhibiting peroxisome proliferator-activated receptor  $\gamma$  expression. *Mol Cell Biol* **31**: 626–638.
- Liu WH, Yeh SH, Chen PJ. 2011. Role of microRNAs in hepatitis B virus replication and pathogenesis. *Biochim Biophys Acta* **1809**: 678–685.
- Liu Q, Yuan B, Lo KA, Patterson HC, Sun Y, Lodish HF. 2012. Adiponectin regulates expression of hepatic genes critical for glucose and lipid metabolism. *Proc Natl Acad Sci* **109**: 14568–14573.
- Liu D, Wu A, Cui L, Hao R, Wang Y, He J, Guo D. 2014. Hepatitis B virus polymerase suppresses NF- $\kappa$ B signaling by inhibiting the activity of IKKs via interaction with Hsp90 $\beta$ . *PLoS One* **9**: e91658.
- Mason AL, Lau JY, Hoang N, Qian K, Alexander GJ, Xu L, Guo L, Jacob S, Regenstein FG, Zimmerman R, et al. 1999. Association of diabetes mellitus and chronic hepatitis C virus infection. *Hepatology* **29**: 328–333.
- Mehta SH, Brancati FL, Sulkowski MS, Strathdee SA, Szklo M, Thomas DL. 2000. Prevalence of type 2 diabetes mellitus among persons with hepatitis C virus infection in the United States. *Ann Intern Med* **133**: 592–599.
- Messeguer X, Escudero R, Farré D, Núñez O, Martínez J, Albà MM. 2002. PROMO: detection of known transcription regulatory elements using species-tailored searches. *Bioinformatics* **18**: 333–334.
- Nakabayashi H, Taketa K, Miyano K, Yamane T, Sato J. 1982. Growth of human hepatoma cells lines with differentiated functions in chemically defined medium. *Cancer Res* **42**: 3858–3863.
- Nassal M. 1992. The arginine-rich domain of the hepatitis B virus core protein is required for pregenome encapsidation and productive viral positive-strand DNA synthesis but not for virus assembly. *J Virol* **66**: 4107–4116.
- Ondracek CR, McLachlan A. 2011. Role of peroxisome proliferator-activated receptor  $\gamma$  coactivator 1 $\alpha$  in AKT/PKB-mediated inhibition of hepatitis B virus biosynthesis. *J Virol* **85**: 11891–11900.
- Ondracek CR, Rushing CN, Reese VC, Oropeza CE, McLachlan A. 2009. Peroxisome proliferator-activated receptor  $\gamma$  Coactivator 1 $\alpha$  and small heterodimer partner differentially regulate nuclear receptor-dependent hepatitis B virus biosynthesis. *J Virol* **83**: 12535–12544.
- Pascual G, Fong AL, Ogawa S, Gamliel A, Li AC, Perissi V, Rose DW, Willson TM, Rosenfeld MG, Glass CK. 2005. A SUMOylation-dependent pathway mediates transrepression of inflammatory response genes by PPAR- $\gamma$ . *Nature* **437**: 759–763.
- Pedersen IM, Cheng G, Wieland S, Volinia S, Croce CM, Chisari FV, David M. 2007. Interferon modulation of cellular microRNAs as an antiviral mechanism. *Nature* **449**: 919–922.
- Puigserver P, Wu Z, Park CW, Graves R, Wright M, Spiegelman BM. 1998. A cold-inducible coactivator of nuclear receptors linked to adaptive thermogenesis. *Cell* **92**: 829–839.
- Qian J, Chen S, Huang Y, Shi X, Liu C. 2013. PGC-1 $\alpha$  regulates hepatic hepcidin expression and iron homeostasis in response to inflammation. *Mol Endocrinol* **27**: 683–692.
- Quasdorff M, Protzer U. 2010. Control of hepatitis B virus at the level of transcription. *J Viral Hepat* **17**: 527–536.
- Ruan H, Pownall HJ, Lodish HF. 2003. Troglitazone antagonizes tumor necrosis factor- $\alpha$ -induced reprogramming of adipocyte gene expression by inhibiting the transcriptional regulatory functions of NF- $\kappa$ B. *J Biol Chem* **278**: 28181–28192.
- Shih CH, Li LS, Roychoudhury S, Ho MH. 1989. In vitro propagation of human hepatitis B virus in a rat hepatoma cell line. *Proc Natl Acad Sci* **86**: 6323–6327.
- Shih C, Yu MY, Li LS, Shih JW. 1990. Hepatitis B virus propagated in a rat hepatoma cell line is infectious in a primate model. *Virology* **179**: 871–873.
- Shlomai A, Paran N, Shaul Y. 2006. PGC-1 $\alpha$  controls hepatitis B virus through nutritional signals. *Proc Natl Acad Sci* **103**: 16003–16008.
- Slagle BL, Andrisani OM, Bouchard MJ, Lee CG, Ou JH, Siddiqui A. 2014. Technical standards for hepatitis B virus X protein (HBx) research. *Hepatology* doi: 10.1002/hep.27360.
- St-Pierre J, Drori S, Uldry M, Silvaggi JM, Rhee J, Jager S, Handschin C, Zheng K, Lin J, Yang W, et al. 2006. Suppression of reactive oxygen species and neurodegeneration by the PGC-1 transcriptional coactivators. *Cell* **127**: 397–408.
- Su F, Schneider RJ. 1996. Hepatitis B virus HBx protein activates transcription factor NF- $\kappa$ B by acting on multiple cytoplasmic inhibitors of rel-related proteins. *J Virol* **70**: 4558–4566.
- Szabo G, Bala S. 2013. MicroRNAs in liver disease. *Nat Rev Gastroenterol Hepatol* **10**: 542–552.
- Tai DJ, Su CC, Ma YL, Lee EH. 2009. SGK1 phosphorylation of I $\kappa$ B Kinase  $\alpha$  and p300 up-regulates NF- $\kappa$ B activity and increases N-Methyl-D-aspartate receptor NR2A and NR2B expression. *J Biol Chem* **284**: 4073–4089.
- Tiollais P, Pourcel C, Dejean A. 1985. The hepatitis B virus. *Nature* **317**: 489–495.
- Tran M, Tam D, Bardia A, Bhasin M, Rowe GC, Kher A, Zsengeller ZK, Akhavan-Sharif MR, Khankin EV, Saintgeniez M, et al. 2011. PGC-1 $\alpha$  promotes recovery after acute kidney injury during systemic inflammation in mice. *J Clin Invest* **121**: 4003–4014.
- Wakui Y, Inoue J, Ueno Y, Fukushima K, Kondo Y, Kakazu E, Obara N, Kimura O, Shimosegawa T. 2010. Inhibitory effect on hepatitis B virus in vitro by a peroxisome proliferator-activated receptor- $\gamma$  ligand, rosiglitazone. *Biochem Biophys Res Commun* **396**: 508–514.

- Wang H, Ryu WS. 2010. Hepatitis B virus polymerase blocks pattern recognition receptor signaling via interaction with DDX3: Implications for immune evasion. *PLoS Pathog* **6**: e1000986.
- Waris G, Huh KW, Siddiqui A. 2001. Mitochondrially associated hepatitis B virus X protein constitutively activates transcription factors STAT-3 and NF- $\kappa$ B via oxidative stress. *Mol Cell Biol* **21**: 7721–7730.
- Wilson R, Warner N, Ryan K, Selleck L, Colledge D, Rodgers S, Li K, Revill P, Locarnini S. 2011. The hepatitis B e antigen suppresses IL-1 $\beta$ -mediated NF- $\kappa$ B activation in hepatocytes. *J Viral Hepat* **18**: e499–e507.
- Wingender E, Chen X, Hehl R, Karas H, Liebich I, Matys V, Meinhardt T, Prüss M, Reuter I, Schacherer F. 2000. TRANSFAC: An integrated system for gene expression regulation. *Nucleic Acids Res* **28**: 316–319.
- Xia L, Tian D, Huang W, Zhu H, Wang J, Zhang Y, Hu H, Nie Y, Fan D, Wu K. 2012. Upregulation of IL-23 expression in patients with chronic hepatitis B is mediated by the HBx/ERK/NF- $\kappa$ B pathway. *J Immunol* **188**: 753–764.
- Yan H, Zhong G, Xu G, He W, Jing Z, Gao Z, Huang Y, Qi Y, Peng B, Wang H, et al. 2012. Sodium taurocholate cotransporting polypeptide is a functional receptor for human hepatitis B and D virus. *eLife* **1**: e00049.
- Yang CC, Huang EY, Li HC, Su PY, Shih C. 2014. Nuclear export of human hepatitis B virus core protein and pregenomic RNA depends on the cellular NXF1-p15 machinery. *PLoS One* **9**: e106683.
- Yoon JC, Puigserver P, Chen G, Donovan J, Wu Z, Rhee J, Adelmant G, Stafford J, Kahn CR, Granner DK, et al. 2001. Control of hepatic gluconeogenesis through the transcriptional coactivator PGC-1. *Nature* **413**: 131–138.
- Yoon S, Jung J, Kim T, Park S, Chwae YJ, Shin HJ, Kim K. 2011. Adiponectin, a downstream target gene of peroxisome proliferator-activated receptor  $\gamma$ , controls hepatitis B virus replication. *Virology* **409**: 290–298.
- Yu X, Mertz JE. 2001. Critical roles of nuclear receptor response elements in replication of hepatitis B virus. *J Virol* **75**: 11354–11364.
- Yu S, Matsusue K, Kashireddy P, Cao WQ, Yeldandi V, Yeldandi AV, Rao MS, Gonzalez FJ, Reddy JK. 2003. Adipocyte-specific gene expression and adipogenic steatosis in the mouse liver due to peroxisome proliferator-activated receptor  $\gamma$ 1 (PPAR $\gamma$ 1) overexpression. *J Biol Chem* **278**: 498–505.
- Zhang X, Daucher M, Armistead D, Russell R, Kottlilil S. 2013. MicroRNA expression profiling in HCV-infected human hepatoma cells identifies potential anti-viral targets induced by interferon- $\alpha$ . *PLoS One* **8**: e55733.
- Zhou R, Hu G, Gong AY, Chen XM. 2010a. Binding of NF- $\kappa$ B p65 subunit to the promoter elements is involved in LPS-induced transactivation of miRNA genes in human biliary epithelial cells. *Nucleic Acids Res* **38**: 3222–3232.
- Zhou Y, Wang S, Ma JW, Lei Z, Zhu HF, Lei P, Yang ZS, Zhang B, Yao XX, Shi C, et al. 2010b. Hepatitis B virus protein X-induced expression of the CXC chemokine IP-10 is mediated through activation of NF- $\kappa$ B and increases migration of leukocytes. *J Biol Chem* **285**: 12159–12168.